AgriEngineering

MDPI

Article

Effect of Green Roofs on the Thermal Environment of Prototype Broiler Houses

Maria Angela de Souza [1], Fernanda Campos de Sousa [1,*], Alex Lopes da Silva [2], Thauane Cordeiro Soares [2], Charles Paranhos Oliveira [1], Ricardo Brauer Vigoderis [3], Fernando da Costa Baêta [1] and Ilda de Fátima Ferreira Tinôco [1]

[1] Department of Agricultural Engineering, Federal University of Viçosa, Viçosa 36570-900, MG, Brazil; maria.a.souza@ufv.br (M.A.d.S.); charles.paranhos@ufv.br (C.P.O.); baeta@ufv.br (F.d.C.B.); iftinoco@ufv.br (I.d.F.F.T.)

[2] Department of Animal Science, Federal University of Viçosa, Viçosa 36570-900, MG, Brazil; alex.lopes@ufv.br (A.L.d.S.); thauane.soares@ufv.br (T.C.S.)

[3] Department of Agricultural Engineering, Federal University of Agreste of Pernambuco, Garanhuns 55292-270, PE, Brazil; ricardo.vigoderis@ufape.edu.br

* Correspondence: fernanda.sousa@ufv.br; Tel.: +55-31998952772

Abstract: The management of thermal environments in animal production facilities presents significant challenges, requiring continuous adjustments to meet animals' physiological needs. This study evaluated the effects of green roofs on the thermal environment and comfort indices in small-scale poultry house prototypes, comparing facilities with and without green roof installations. The research tested various roof types (ceramic, fiber cement, and metal) combined with emerald grass (*Zoysia japonica*) green roof systems. Parameters measured included air temperature, relative humidity, internal roof surface temperature, Temperature and Humidity Index (THI), Black Globe Humidity Index (BGHI), Human Comfort Index (HCI), and Thermal Radiation Load (TRL) under both open and closed conditions. Results showed that green roofs reduced indoor air temperature by up to 2.4 °C in open prototypes and 10.6 °C in closed prototypes during peak heat periods. In combinations using green roofs with fiber cement tiles, internal roof surface temperature decreased by 24.0 °C in open prototypes and 27.0 °C in closed configurations. The implementation of green roofs resulted in THI reductions of 2.3 and 8.1 units in open and closed prototypes, respectively, BGHI decreases of 2.8 and 11.3 units, and TRL reductions of 21.0 W/m^2 and 74.0 W/m^2. HCI measurements confirmed improved thermal comfort conditions with green roof installations in both settings. This study concludes that green roofs effectively enhance the thermal environment by reducing bioclimatic indices during hot periods while maintaining stable conditions during cooler weather, thereby improving overall thermal comfort in animal facilities.

Keywords: animal ambience; animal welfare; rural constructions; thermal stress

Academic Editor: In-Bok Lee

Received: 11 November 2024
Revised: 4 January 2025
Accepted: 10 January 2025
Published: 14 January 2025

Citation: Souza, M.A.d.; Sousa, F.C.d.; Silva, A.L.d.; Soares, T.C.; Oliveira, C.P.; Vigoderis, R.B.; Baêta, F.d.C.; Tinôco, I.d.F.F. Effect of Green Roofs on the Thermal Environment of Prototype Broiler Houses. *AgriEngineering* **2025**, 7, 16. https://doi.org/10.3390/agriengineering7010016

1. Introduction

Brazilian poultry farming stands out in the animal production sector through the continuous development and implementation of advanced technologies that enhance productive efficiency while reducing operational costs [1]. With an accumulated growth exceeding 1.087% in chicken meat production, Brazil has established itself as the second-largest producer and primary global exporter, solidifying its leadership position in the international market [2]. However, despite the robust expansion of the poultry sector, significant knowledge gaps persist regarding thermal conditioning in tropical poultry facilities, particularly concerning energy consumption, heating and cooling systems efficiency, animal welfare, and air quality [3]. Consequently, while addressing the increasing demand for animal protein, the fundamental challenge of maintaining optimal thermal comfort for animals throughout the production cycle remains paramount. Thermal comfort constitutes a critical factor for both welfare and productive performance in intensive farming systems [4,5].

In response to accelerated climate change, regions experience elevated temperatures, increased precipitation variability, and intensified frequency of extreme weather events. The convergence of climate change impacts and escalating livestock production demand needs to increase production sustainably while minimizing environmental impacts [6–8]. Considering climate's substantial influence on animal production, implementing innovative construction alternatives and ambiance strategies becomes essential to ensure thermal and energy efficiency in facilities [9,10]. These strategies encompass strategic shading implementation, selection of high thermal capacity materials for heat regulation, and adoption of advanced heating mitigation technologies. Such comprehensive measures optimize internal thermal conditions, enhancing facility sustainability while minimizing environmental impact and energy consumption, simultaneously ensuring animal welfare. Within this framework, agricultural facilities' roofing emerges as a crucial element, playing an instrumental role in controlling solar radiation and buildings' thermal load [4,11]. To establish an optimal thermal environment, a comprehensive understanding of roofing materials' thermal properties becomes essential, facilitating enhanced heat exchange dynamics in buildings [12,13].

In this context, green roof technology represents an innovative construction approach that has gained significant recognition in scientific research and the construction sector due to its comprehensive social, environmental, and economic benefits [14]. Green roof systems serve as an effective strategy for optimizing buildings' thermal comfort, offering substantial advantages in both hot and cold climates. In hot climates, these systems effectively reduce internal thermal load, while in cold climates, they facilitate heat retention, thereby maintaining optimal thermal comfort [15–17]. The moisture retention capacity of green roof systems plays a fundamental role in reducing surface temperature and enhancing cooling efficiency through evapotranspiration, particularly during summer periods. Cooling efficiency is predominantly influenced by substrate thickness and vegetation cover density. The plant canopy functions as a natural radiation shield, significantly reducing solar radiation transmission to the roof surface, consequently lowering the surface temperature and diminishing building cooling requirements. The canopy structure further modulates heat exchange processes, as foliar surfaces reflect, transmit, and absorb solar radiation, thereby regulating the system's thermal dynamics [18]. Beyond its thermal insulation properties, the green roof system orchestrates solar radiation balance through convection, evaporation, and heat conduction mechanisms, reflecting 20% to 30% of solar radiation, using up to 60% for photosynthetic processes, and facilitating evaporative cooling. The system's thermal efficiency correlates with substrate depth variations while additionally contributing significantly to rainwater management optimization [19–22].

Evidence suggests that green roof systems possess considerable potential for mitigating animal production impacts within the context of global climate change while simultaneously reducing the effects of elevated air temperatures on animal production systems. However, existing literature predominantly focuses on green roof applications in urban buildings [10,16,18,19,21,23–30]. This urban-centric focus constrains understanding of green roof potential in alternative contexts, particularly animal production environments [31,32]. Implementing green roof systems in rural settings, specifically animal production facilities, offers significant advantages, including enhanced thermal comfort and improved sustainability metrics. Beyond their established positive effects on building thermal conditioning, green roof systems contribute substantially to energy conservation through reduced heating and cooling system demands. Through investigating this technology in a relatively unexplored context, this study provides empirical evidence demonstrating green roofs' impacts on energy efficiency and animal welfare in rural environments. Thermal comfort assessment in agricultural facilities relies on specialized indexes that quantify comfort conditions for both animals and human operators. Among these comprehensive measures, the Temperature and Humidity Index (THI) serves as a primary indicator, evaluating the synergistic effects of temperature and humidity [33,34]. Additionally, the Black Globe Humidity Index (BGHI) incorporates environmental thermal radiation measurements [35], while the Human Comfort Index (HCI) evaluates human well-being through temperature–humidity interactions [36]. To maintain optimal occupational conditions, thermal comfort parameters must adhere to standards established by the Ministry of Labor and Employment [37]. Furthermore, the Radiant Thermal Load (RTL) provides a quantitative measurement of direct radiation impacts on biological systems [38]. These thermal comfort indexes enable comprehensive monitoring of green roofs' effects on thermal comfort conditions for both animals and human operators within production systems.

Furthermore, the utilization of reduced-scale models enables precise prediction of thermal conditions in full-scale installations, accurately simulating environmental thermal behavior. This scaled approach proves particularly valuable for complex investigations, such as those focusing on thermal comfort in animal production, as it facilitates experimental control, optimizes research efficiency, and enhances understanding of underlying physical principles [13,39–41]. Thus, this research investigates green roof effects on the thermal environment of reduced-scale poultry house prototypes, specifically characterizing the thermal environment and thermal comfort indices in poultry house prototypes with and without green roof systems.

2. Materials and Methods

2.1. Experimental Location

This investigation was conducted at the Department of Agricultural Engineering's (DEA) Rural Constructions and Environment Area, Federal University of Viçosa (UFV), located in Viçosa/MG, Brazil. The experiment was carried out from 24 February to 11 March 2022 at the Research Center on Ambience and Engineering of Agro-Industrial Systems (AMBIAGRO), positioned at latitude 20° 45′ south and longitude 45° 52′ west, with an elevation of 670 m. According to the Köppen classification, the local climate is characterized as Cwa, featuring a subtropical pattern with dry, cold winters and hot, humid summers. The experimental phase was conducted during the summer season. Six scale-reduced commercial poultry house prototypes were constructed following a 1:5 scale similarity concept [42]. The prototypes featured identical dimensions: 2.5 m in width and 3.2 m in length, with a ceiling height of 0.6 m and an eave of 0.5 m. These structures were distributed in two parallel rows and positioned on level, grass-covered terrain with an east–west orientation. The eaves of the prototypes were closed with wood.

The poultry houses' prototypes were evaluated under field conditions, without external environmental control, due to the open nature of the experimental area. The experiment was conducted in two distinct phases: in the first, the prototypes were left with an open construction design, while in the second, blue polyethylene side curtains were installed, allowing partial enclosure of the structure. Each experimental condition was maintained for a period of seven days, during which data were systematically collected.

2.2. Vegetation Coverture

Emerald grass (*Zoysia japonica*) represents one of the predominant species used in Brazil for landscaping applications, sports facilities, and ornamental gardens, owing to its exceptional adaptability to tropical climate conditions [43,44]. This species demonstrates superior resistance to foot traffic and minimal maintenance requirements, making it extensively used for ground coverage in transportation infrastructure, public spaces, and residential areas, where its aesthetic appeal and durability are highly valued [45]. These characteristics enhance its suitability for green roof applications [31,46], where it contributes to thermal insulation, water retention, and resource efficiency. The increasing implementation of ornamental grasses in urban and residential environments has established *Zoysia japonica* as the primary selection for landscaping initiatives throughout the country [43].

2.3. Irrigation Management of Vegetation Coverture

Water requirements of the grass coverage were determined based on crop evapotranspiration (ETc) and calculated using the Penman–Monteith method (Equation (1)), following Allen et al. [47]. Reference evapotranspiration (ET0) values were derived from climatic variables (air temperature, relative humidity, atmospheric pressure, wind speed, and radiation) obtained from INMET [48].

$$ETc = ET0 \times Kc \quad (1)$$

where ETc represents crop evapotranspiration, ET0 represents reference evapotranspiration, and Kc represents the crop coefficient.

A Kc value of 1 was implemented for *Zoysia japonica* grass, as established by Madeira et al. [49], given its utilization as a reference species in the evapotranspiration determination model. Reference evapotranspiration (ET0) calculations incorporated climate variables from the preceding irrigation day. This estimation enabled the calculation of crop evapotranspiration for the total grass coverage area, thereby determining daily water requirement, which represented the volume of water applied per day accounting for daily precipitation in the available water depth (Table 1). Manual irrigation was conducted throughout the experimental period, initiating one day before each experimental data collection phase and occurring at three daily intervals, 08:00 A.M., 1:00 P.M., and 6:00 P.M., in accordance with daily water requirements.

Table 1. Daily estimation of water demand for *Zoysia japonica* grass during the summer in Viçosa-MG, based on crop evapotranspiration (ETc) and precipitation.

Day	ETc (mm)	Water Demand ($L \cdot m^{-2} \cdot dia^{-1}$)	Precipitation (mm)
1	4.51	40.59	0.20
2	4.35	39.15	0.00
3	4.23	38.07	0.00
4	4.39	39.51	0.00
5	4.55	40.95	8.40
6	4.46	40.14	0.40
7	4.22	37.98	0.00
8	4.81	43.29	0.00
9	4.53	40.77	0.00
10	4.45	40.05	0.00
11	4.55	40.95	0.00
12	4.50	40.50	0.00
13	4.29	38.61	0.20
14	4.55	40.95	0.20
15	3.29	29.61	1.40
16	4.50	40.50	0.00

Source: Authors, based on INMET data [48].

2.4. Types of Tested Roofing Materials

The experimental treatments comprised three different roofing material combinations, evaluated both with and without green roof systems. The roofing materials tested included Roman ceramic tile (CT), corrugated fiber cement tile (FCT), and trapezoidal metallic tile (MT). Three of the six prototypes incorporated each roofing material type in conjunction with a green roof system using *Zoysia japonica* grass. The investigation encompassed two experimental phases evaluating distinct building typologies: open and closed prototypes. The closed prototype configuration featured blue polyethylene curtains installed along the longitudinal sides of the structures (Figure 1).

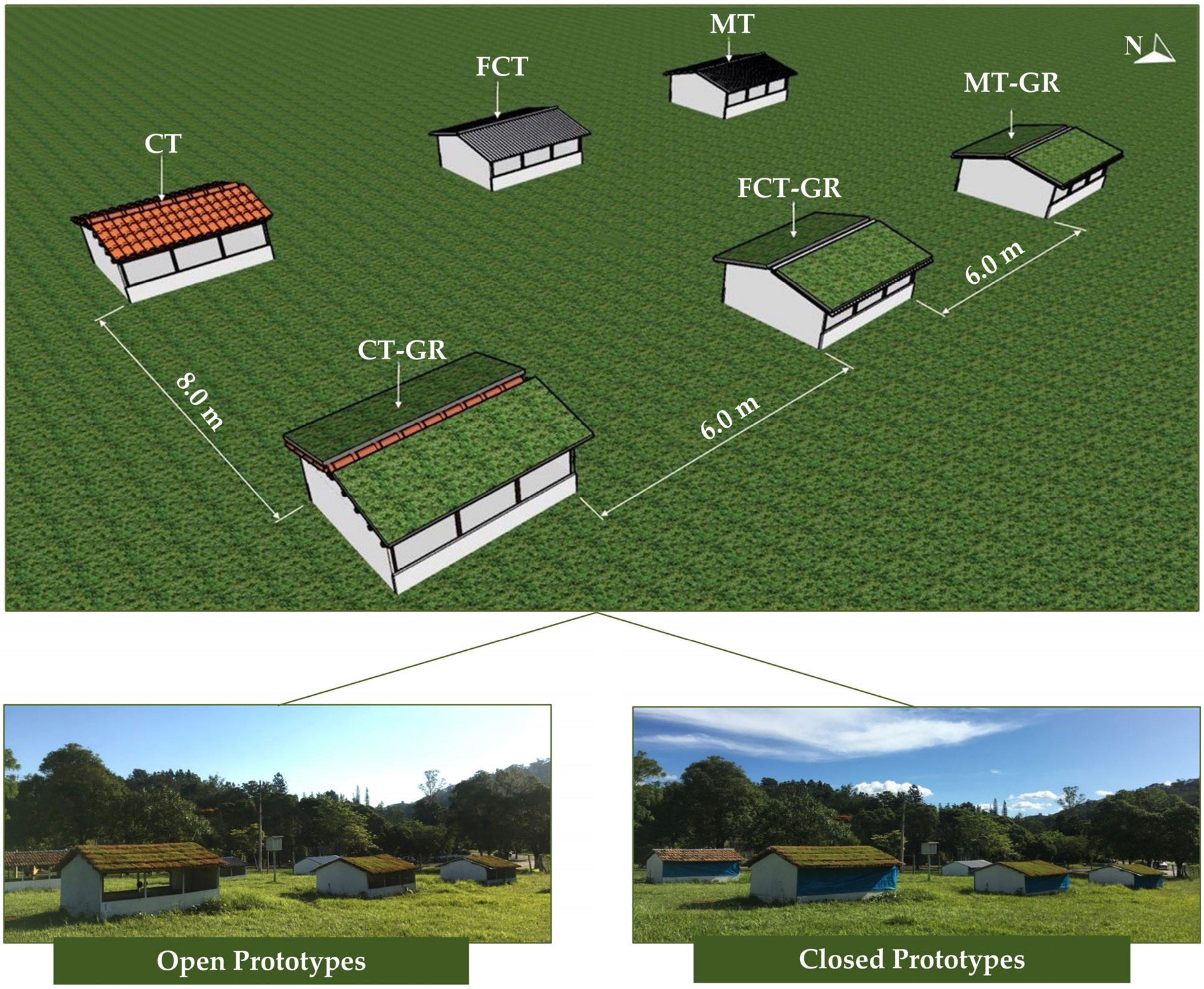

Figure 1. Representation of the positioning of prototypes in the experimental area, with different treatments: prototype with ceramic tile (CT), prototype with fiber cement tile (FCT), prototype with metal tile (MT), prototype with ceramic tile and green roof (CT-GR), prototype with fiber cement tile and green roof (FCT-GR), and prototype with metal tile and green roof (MT-GR). Emphasizing the different constructive typologies, with open prototypes and closed prototypes. Source: Authors.

Before the experimental period, ceramic and fiber cement tiles underwent thorough cleaning procedures. Subsequently, these materials received varnish waterproofing treatment to prevent moisture infiltration. The green roof installation process included the use of a black shade cloth, which served as a support for the substrate, facilitating the uniform distribution of the grass over the roof surface. Each prototype had a coverage area of 9 m^2, with a thickness of 8 cm/m^2 and a grass density of 26 kg/m^2. In addition, the fiber cement tiles used in this study had moderately darkened surface characteristics due to previous exposure, which may have increased their heat absorption capacity compared to new materials.

2.5. Characterization of the Thermal Environment of the Prototypes

The internal thermal environment of each prototype underwent systematic monitoring through continuous temperature and relative humidity measurements. Monitoring used Onset® dataloggers (model HOBO UX100-03; Onset Computer Corporation, Bourne, MA, USA), equipped with temperature measurement capabilities ranging from −20.0 °C to +70.0 °C (accuracy: ±0.21 °C; resolution: ±0.024 °C) and relative humidity measurement capabilities spanning 15.0% to 95.0% (accuracy: ±3.5%; resolution: 0.07%). Two sensors, positioned at each prototype's geometric center, facilitated continuous internal environment monitoring. Data acquisition occurred at minute intervals throughout the 24 h cycle during the entire experimental period. One sensor recorded dry-bulb temperature (air temperature) and relative humidity, enabling dew point temperature calculation, while a second sensor, positioned within a black globe, measured black globe temperature. Additionally, air velocity measurements were obtained at each prototype's geometric center using a TAFR-200 hot-wire anemometer (measurement range: 0.1 to 25.0 m/s; resolution: 0.01 m/s; accuracy: 5%; Wöhler Technik GmbH, Bad Wünnenberg, Germany). For treatment analysis evaluating various covering materials with and without green roof systems, internal surface temperature measurements of prototype roofs were obtained using a Fluke® infrared thermometer (model 62 MAX; Fluke Corporation, Everett, WA, USA). This instrument featured a measurement range of –30.0 °C to +500.0 °C (accuracy: ±1.5 °C; resolution: 0.1 °C). Surface temperature determination occurred from an internal geometric reference point, measured at 0.5 m distance, with emissivity adjustments corresponding to specific covering material (Table 2). The measurements were conducted at 3 h intervals throughout the 24 h cycle during the experimental period.

Table 2. Emissivity values of the surface temperature sensor of different roofing materials.

Coverture Material	Emissivity (£)
Ceramic tile	0.85–0.95
Fiber Cement Roof Tile	0.92
Metal Roof Tile	0.25
Green Roof (Grass)	0.90

Source: Adapted from Baêta and Souza [11].

The characterization of the external thermal environment of the prototypes in the experimental area was performed by determining the air temperature and relative humidity values throughout the entire experimental period using data from the National Institute of Meteorology [48]. Descriptive statistical analyses were performed to calculate the mean, minimum, and maximum values of air temperature and relative humidity in the external environment.

2.6. Characterization of Thermal Comfort Indexes

The effects of treatments, encompassing various roofing materials with and without green roof systems, on the prototype's thermal comfort, were evaluated using established bioclimatological indexes. These metrics, extensively validated and widely implemented in scientific investigations [31,36,50–56], enable precise analysis of thermal comfort conditions for both animals and workers in animal production facilities. Their demonstrated effectiveness in characterizing poultry environments underscores their relevance in assessing covering material impacts and optimizing thermal conditions in poultry facilities. The THI was calculated using the model developed by Thom [33] and refined by Mader et al. [34], incorporating air temperature and relative humidity parameters (Equation (2)).

$$THI = 0.8 \times T_d + (RH/100) \times (T_d - 14.4) + 46.4 \quad (2)$$

where T_d represents the dry bulb temperature (°C), and RH represents the relative humidity of the air (%).

The (BGHI) was determined using Equation (3), established by Buffington et al. [35], using black globe temperature and dew point temperature measurements.

$$BGHI = T_{bg} + 0.36\ T_{dp} + 41.5 \quad (3)$$

where T_{bg} represents the black globe temperature (°C), and T_{dp} represents the dew point temperature (°C).

The HCI developed by Rosenberg [36] was determined and calculated using Equation (4), incorporating air temperature, relative humidity, vapor pressure (Equation (5)), and saturated air vapor pressure (Equation (6)).

$$HCI = T_a + \frac{5}{9}(e_a - 10) \quad (4)$$

$$e_a = \frac{(e_s \times RH)}{100} \quad (5)$$

$$e_s = 0.611 \times 10^{\left\lfloor \frac{7.5 \times T_a}{237.3 + T_a} \right\rfloor} \quad (6)$$

where T_a represents the air temperature (°C), RH represents the relative humidity of the air (%), e_a represents the vapor pressure (kPa), and e_s represents the saturated air vapor pressure (kPa).

The RTL established by Kelly and Bond [38] was determined based on the radiant thermal exchanges of the roof and calculated using Equation (7) through the Stefan–Boltzmann constant and the mean radiant temperature (MRT) values, as presented in Equation (8).

$$RTL = \sigma MRT^4 \quad (7)$$

where σ represents the Stefan-Boltzmann constant, $W \cdot (m^2 \cdot K^4)^{-1}$, and MRT represents the mean radiant temperature, (K).

$$MRT = 100\left(2.51\sqrt{V}\left(T_{bg} - T_d\right) + \left(\frac{T_{bg}}{100}\right)^4\right)^{\frac{1}{4}} \quad (8)$$

where V represents the air velocity ($m \cdot s^{-1}$), T_{bg} represents the black globe temperature (K), and T_d represents the dry bulb temperature (K).

To assess the thermal comfort of animals and humans, the calculated values of air temperature, relative humidity, THI, BGHI, and HCI were compared with the comfort ranges described in the literature, as presented in Table 3.

Table 3. Thermal comfort ranges for broilers (air temperature, relative humidity, THI, and BGHI) and workers (HCI).

Comfort Range	Week of Life					Authors
	1	2	3	4	5	
Air temperature (°C)	32.3–35.0	26.4–32.0	21.6–29.0	21.6–26.0	20.0–23.0	Silva et al. [51] and Oliveira et al. [53]
Relative humidity (%)	56.90	64.40	68.50	68.50	69.20	Oliveira et al. [53]

Table 3. *Cont.*

Comfort Range	Week of Life					Authors
	1	2	3	4	5	
THI	72.4–80.0	68.4–76.0	64.5–72.0	60.5–68.0	56.6–64.0	Silva et al. [51]
BGHI	81.30	74.90	69.80	69.80	68.70	Oliveira et al. [53]
HCI			20.0–29.0 *			Santos [57], Souza et al. [58] and Santos et al. [59]

* Values for humans. Source: Adapted by authors.

2.7. Statistical Analyses

The entire dataset underwent statistical analysis using the Generalized Least Squares (GLS) procedure implemented in R statistical software version 4.1.3 [59]. The analytical framework incorporated the evaluation of multiple factors: roofing tile type, presence or absence of green roof systems, data collection timing, and their respective interactions. The temporal component of data collection was integrated into the model as a repeated measure, with an evaluation of multiple covariance structures, including compound symmetry, heterogeneous compound symmetry, first-order autoregressive, and heterogeneous first-order autoregressive matrices. The selection of the optimal covariance matrix structure was determined based on the minimization of the Akaike Information Criterion (AIC). The heterogeneous first-order autoregressive matrix demonstrated a superior fit and was subsequently implemented across all analyses. Mean separation procedures, when warranted by significant effects, were conducted using Tukey's multiple comparison test at a 0.05 probability threshold. In instances where significant interactions were detected, these were subjected to detailed decomposition analysis.

3. Results

3.1. Open Prototyping Environments

3.1.1. External Environment

The external environment in the open prototype experimental area was characterized using temperature and relative humidity data from INMET [48] over the seven-day experimental period, allowing the characterization of external thermal variations (Figure 2). The data revealed a well-defined daily cycle: air temperatures are lowest at dawn (16.0 °C to 19.0 °C), gradually increasing throughout the morning and reaching peak values between 26.0 °C and 30.0 °C from 12 P.M. to 3 P.M. Conversely, relative humidity exhibited an opposite pattern, with the high values at dawn (95% to 98%) and decreasing to 40% to 60% during the hottest afternoon hours (3 P.M.). This inverse relationship between temperature and relative humidity indicates that the external environment becomes drier as air temperature rises, particularly during the afternoon hours.

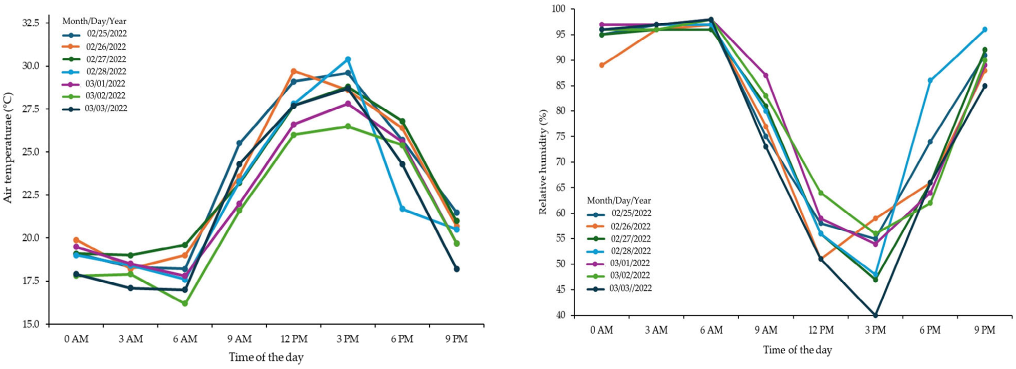

Figure 2. Characterization of the external thermal environment with temperature and relative humidity data during the experimental period with open prototypes in Viçosa-MG. Source: Adapted from INMET [48].

3.1.2. Thermal Environment

The open prototype experiments revealed significant differences (p-value < 0.0001) across all analyzed variables, including air temperature, internal surface temperature, and relative humidity, for the three types of roof tiles tested, both with and without green roofs, throughout the observation period (Figure 3). Statistical analysis of air temperature data showed a significant (p-value < 0.0001) simple interaction effect of time and a double interaction effect between green roof presence and time (Figure 3A).

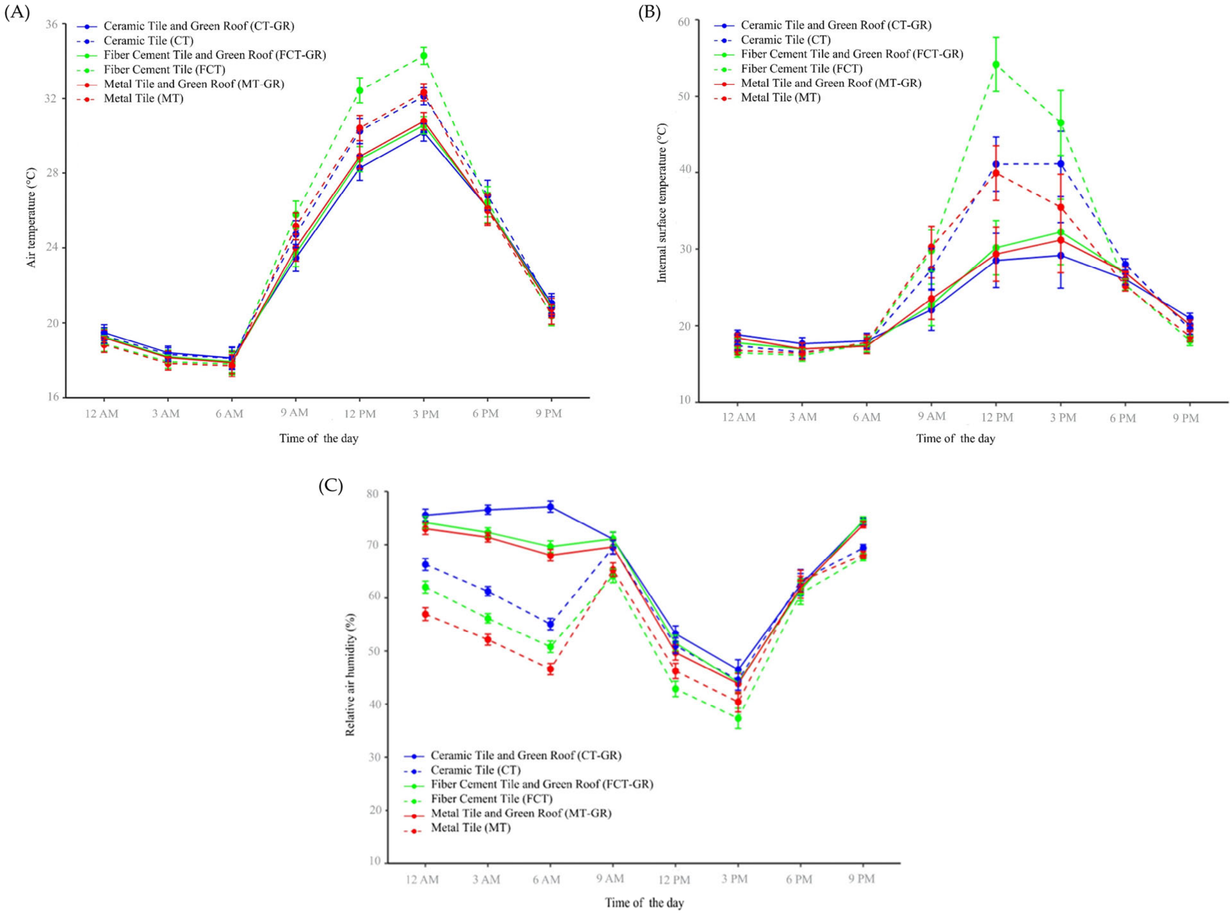

Figure 3. Behavior of air temperature (**A**), internal surface temperature (**B**), and relative humidity (**C**) in open prototypes, showing different types of roof tiles, with and without the presence of a green roof, at different times. Source: Authors.

Evaluation of internal surface temperature in open prototypes (Figure 3B) revealed a significant simple interaction effect (p-value < 0.0001) for both time and green roof presence, along with a double interaction between these factors. Similarly, relative humidity data indicated a significant interaction effect (p-value < 0.0001) for time, roof tile type, and green roof presence (Figure 3C), with additional double interactions observed between green roof and time and between roof tile type and time. These findings demonstrate the influence of roof tile type and green roof presence on thermal regulation and humidity levels under open prototype conditions.

Air temperature analysis in open prototypes, both with and without green roofs, revealed statistically significant differences at 9:00 A.M., 12:00 P.M., and 3:00 P.M., with higher air temperature recorded in prototypes without green roofs (Figure 3A). This finding highlights the substantial impact of green roofs on the thermal environment, particularly during peak external temperature periods when increased energy consumption is typically required to maintain optimal thermal conditions. Figure 3A demonstrates that prototypes with green roofs exhibited lower air temperatures compared to those without, showing an average reduction of 2.4 °C at both 12:00 P.M. and 3:00 P.M. during the hottest parts of the day.

Internal surface temperature data on roofing materials in open prototypes (Figure 3B) showed statistically significant differences (p-value < 0.0001) only at 3:00 P.M. and 9:00 P.M. The highest internal surface temperature was recorded in the prototype with fiber cement tiles without a green roof. The presence of green roofs resulted in substantial temperature reductions: 24.0 °C for fiber cement tiles, 12.6 °C for ceramic tiles, and 10.5 °C for metallic tiles.

Relative humidity analysis open prototypes (Figure 3C) revealed statistically significant differences (p-value < 0.0001) at most time points, with the exception of 9:00 A.M., 6:00 P.M., and 9:00 P.M. The highest relative humidity values were observed in prototypes with ceramic tiles during the cooler periods (9:00 P.M. to 6:00 A.M.), while the lowest values were recorded in prototypes with fiber cement tiles during the warmer hours (9:00 A.M. to 6:00 P.M.). Notably, prototypes with green roofs consistently maintained higher relative humidity levels, remaining above 70.0% between 9:00 P.M. and 6:00 A.M., corresponding with lower air temperatures.

3.1.3. Thermal Comfort

Open prototype experiments demonstrated significant variations (p-value < 0.0001) in thermal comfort indexes among the three types of roof tiles tested, with and without green roofs, throughout the observation period (Figure 4).

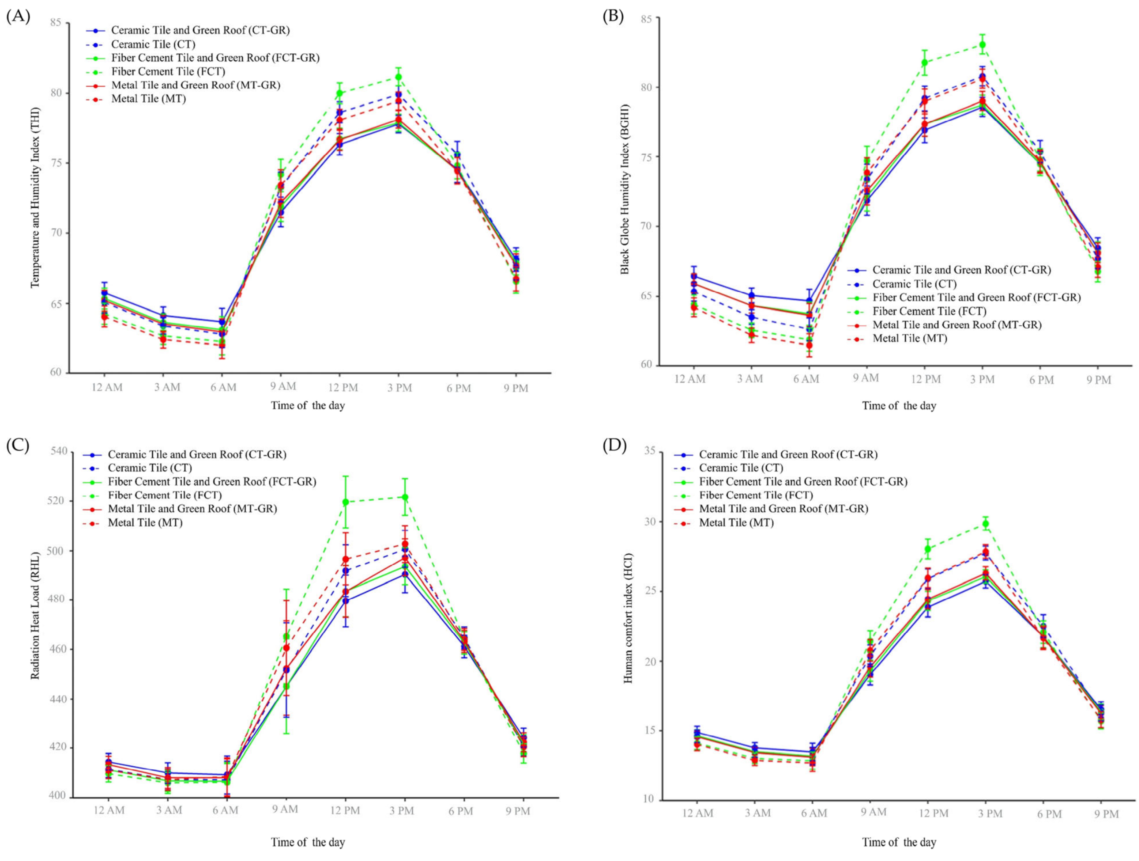

Figure 4. The behavior of the THI (**A**), BGHI (**B**), RTL (**C**), and HCI (**D**) in open prototypes demonstrating the effects of different types of roofing tiles, both with and without the presence of a green roof, at various time points. Source: Authors.

Statistical analysis of THI data in open prototypes (Figure 4A) revealed significant effects (p-value < 0.0001): a simple interaction with times of day and a double interaction between green roof presence and time of day. Similarly, BGHI data analysis (Figure 4B) showed significant simple interaction effects with time of day and double interaction effects between green roof presence and time of day (p-value < 0.0001). RTL data analysis (Figure 4C) identified significant simple interaction effects with time of day (p-value < 0.0001) and double interaction effects between green roof presence and time of day. HCI analysis in open prototypes (Figure 4D) revealed significant simple interaction effects with time of day and green roof presence, along with significant double interaction effects (p-value < 0.0001). These results demonstrate how temporal variation and green roof presence influence thermal comfort indexes in prototypes. THI analysis in open prototypes revealed statistically significant differences at 9:00 A.M., 12:00 P.M., and 3:00 P.M., with higher values in prototypes without green roofs, particularly those with fiber cement tiles (Figure 4A). At 3:00 P.M., green roof presence contributed to a THI reduction of 2.3 across all tile types. During nighttime hours (9:00 P.M. to 6:00 A.M.), prototypes with green roofs across all had higher average THI values than those without.

BGHI analysis in open prototypes showed that green roof presence did not produce statistically significant differences at 6:00 P.M. and 9:00 P.M. However, during peak temperature periods (12:00 P.M. and 3:00 P.M.), prototypes without green roofs exhibited elevated BGHI values, particularly those with fiber cement tiles (Figure 4B).

RTL data analysis in open prototypes revealed statistically significant differences (p-value < 0.0001) at 12:00 P.M. and 3:00 P.M. Prototypes showed that green roofs showed higher RTL averages during peak heat periods (9:00 A.M. to 3:00 P.M.), particularly those with fiber cement roofing (Figure 4C). During nighttime hours (6:00 P.M. to 6:00 A.M.), ceramic tiles with green roofs provided superior thermal insulation, maintaining higher RTL values compared to other treatments.

HCI analysis in open prototypes showed significant differences (p-value < 0.0001) at 9:00 A.M., 12:00 P.M., and 3:00 P.M. regarding green roof presence. For tile type, significant differences (p-value < 0.0001) were observed at 3:00 P.M. Prototypes without green roofs exhibited higher average HCI values during peak heat periods, with fiber cement tiles showing the highest HCI (Figure 4D). During nighttime (6:00 P.M. to 6:00 A.M.), ceramic tiles with green roofs demonstrated enhanced thermal insulation, maintaining higher HCI averages than other treatments.

3.2. Closed Prototyping Environments

3.2.1. External Environment

The external environment in the closed prototype experimental area was characterized using temperature and relative humidity data from INMET [48] over the seven-day experimental period, enabling the description of external thermal variations (Figure 5). Air temperature data showed minimum values at dawn, ranging from 17.5 °C to 21.2 °C, while peak values occurred in the afternoon between 26.1 °C and 30.0 °C. Relative humidity reached its highest levels in the early morning hours, ranging from 92% to 98%, and decreased throughout the day, reaching minimum values of 47% to 66% during peak temperature periods (12 P.M. and 3 P.M.). These data demonstrate an inverse relationship between temperature and relative humidity, where temperature increases correspond to decreases in relative humidity levels.

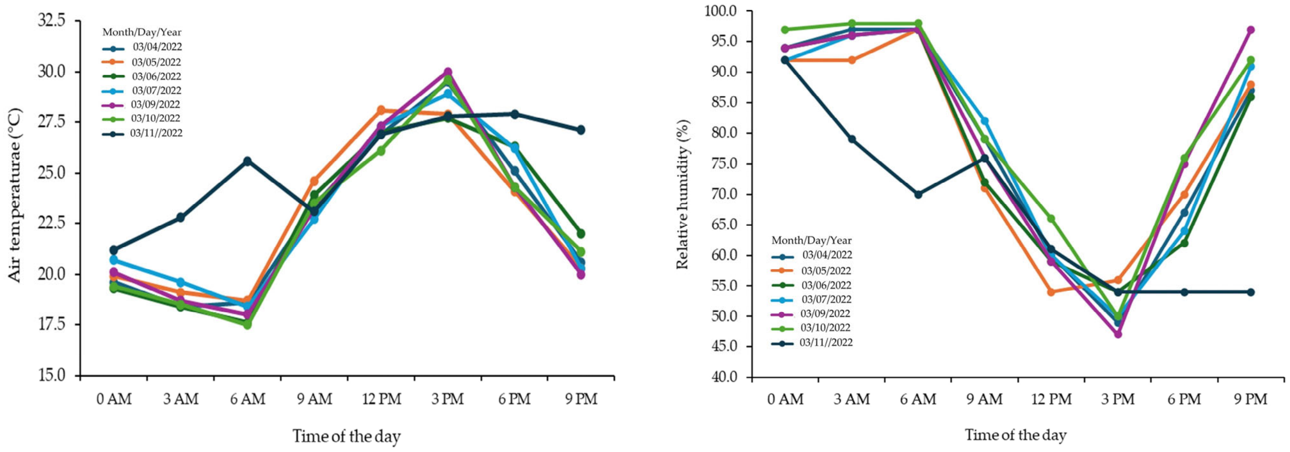

Figure 5. Characterization of the external thermal environment with temperature and relative humidity data during the experimental period with closed prototypes in Viçosa-MG. Source: Adapted from INMET [48].

3.2.2. Thermal Environment

The closed prototypes showed significant differences (p-value < 0.0001) across all analyzed thermal variables, including air temperature, internal surface temperature, and relative humidity. These differences were observed among the three types of roof tiles, both with and without green roofs, throughout the observation period (Figure 6).

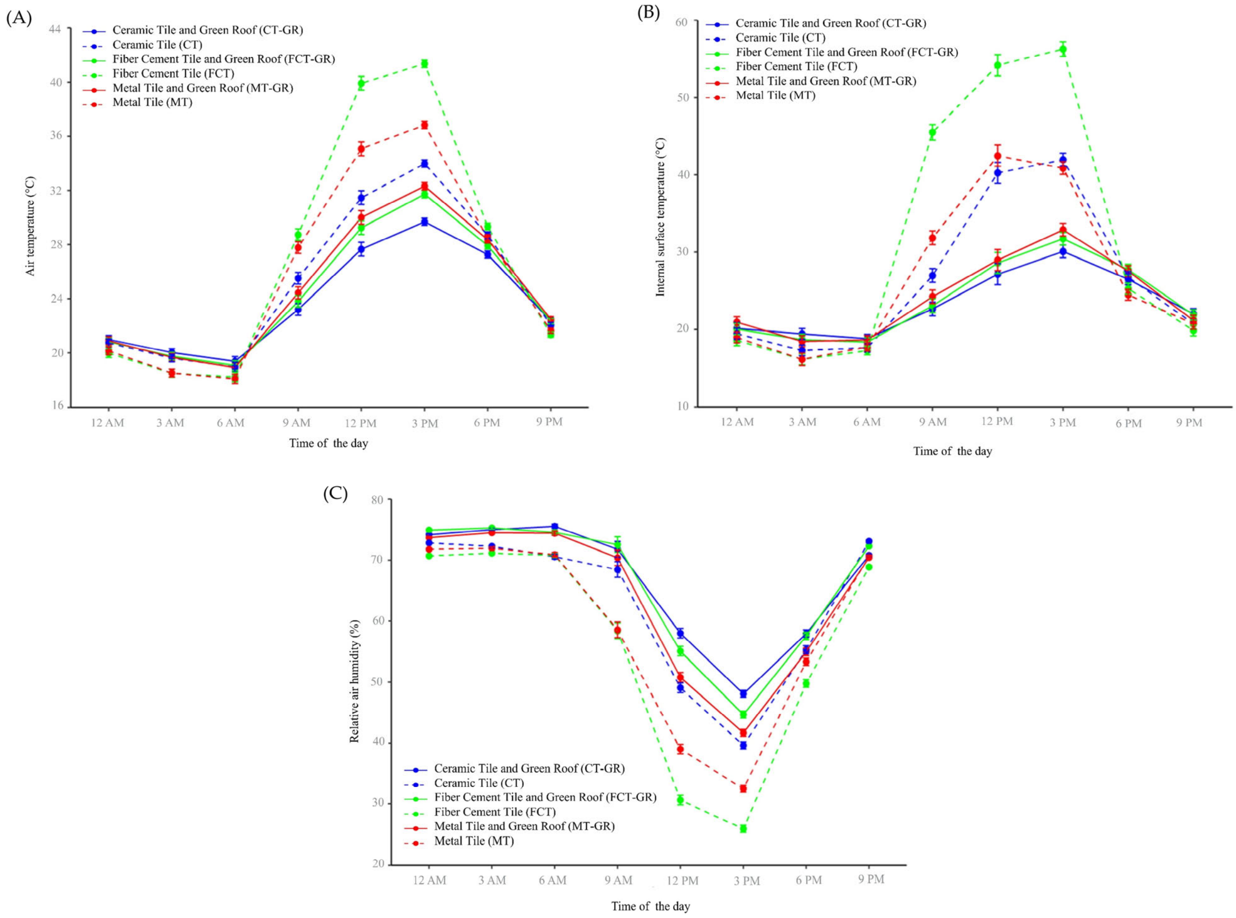

Figure 6. Behavior of air temperature (**A**), internal surface temperature (**B**), and relative humidity (**C**) in closed prototypes, showing different types of roof tiles, with and without the presence of a green roof, at different times. Source: Authors.

Statistical analysis of air temperature data from the closed prototype experiment (Figure 6A) revealed significant simple, double, and triple interactions (p-value < 0.0001). Similarly, internal surface temperature analysis (Figure 6B) showed significant effects (p-value < 0.0001) across all interaction types. The relative humidity data analysis (Figure 6C) also demonstrated significant interactions (p-value < 0.0001) among all variables. Consequently, each interaction was examined individually to thoroughly investigate significant effects across different time points.

In closed prototypes (Figure 6A), significant interactions (p-value < 0.0001) were observed among all variables regarding internal air temperature values. The presence of green roofs resulted in substantial reductions in mean air temperature, particularly during peak heat periods. At 12:00 P.M., temperature reductions were 10.6 °C for fiber cement tiles, 5.1 °C for metallic tiles, and 3.8 °C for ceramic tiles. While no statistically significant temperature differences were found at 12:00 A.M. and 6:00 A.M., green roofs provided thermal damping during cooler periods (9:00 P.M. to 6:00 A.M.), with notable effects at 3:00 A.M., particularly in prototypes with metal tiles.

Surface temperature analysis in closed prototypes (Figure 6B) revealed significant interactions (p-value < 0.0001) at 9:00 A.M. and 3:00 P.M. Green roof presence significantly reduced surface temperatures at 3:00 P.M.: 24.6 °C for fiber cement tiles, 8.0 °C for metallic tiles, and 11.9 °C for ceramic tiles. While no significant differences were observed at 9:00 P.M., 12:00 A.M., and 6:00 A.M., green roofs exhibited a damping effect during cooler hours, with a statistically significant difference at 3:00 A.M.

Relative humidity analysis in closed prototypes (Figure 6C) showed significant interactions (p-value < 0.0001) among all variables, with statistically significant differences at all time points. Green roof presence led to substantial increases in mean relative humidity, particularly at 3:00 P.M.: 18.7% in prototypes with fiber cement tiles, 9.2% with metal tiles, and 8.5% with ceramic tiles. These increases can be attributed to the prototypes' closed lateral sides, which limited natural ventilation and consequently affected thermal exchanges.

3.2.3. Thermal Comfort

The closed prototype experiments revealed significant differences (p-value < 0.0001) in thermal comfort indexes across all three roof tile types, both with and without green roofs, throughout the observation period (Figure 7).

Statistical analysis of THI data (Figure 7A) showed significant simple, double, and triple interaction effects (p-value < 0.0001) across nearly all analyzed variables. Similarly, BGHI data analysis (Figure 7B) revealed significant effects (p-value < 0.0001) from simple interactions with time, double interactions between tile type and time, green roof and time, as well as triple interactions among time, tile type, and green roof presence. RTL data analysis in closed prototypes (Figure 7C) demonstrated significant effects (p-value < 0.0001) in simple, double, and triple interactions across all tested variables. HCI data analysis (Figure 7D) also demonstrated significant simple, double, and triple interaction effects (p-value < 0.0001) among all variables. Each interaction was analyzed separately to evaluate effects across different times of day.

In closed prototypes (Figure 7A), significant interactions were observed across almost all analyzed variables. At 3:00 P.M., green roof presence led to substantial THI reductions: 7.0 for fiber cement tiles, 3.8 for ceramic tiles, and 3.5 for metal tiles. Prototypes without green roofs exhibited the highest average THI values at 12:00 P.M. and 3:00 P.M., particularly those with fiber cement and metal tiles, attributed to the thermal properties of these materials. Conversely, prototypes with green roofs maintained lower THI values, especially those with ceramic tiles.

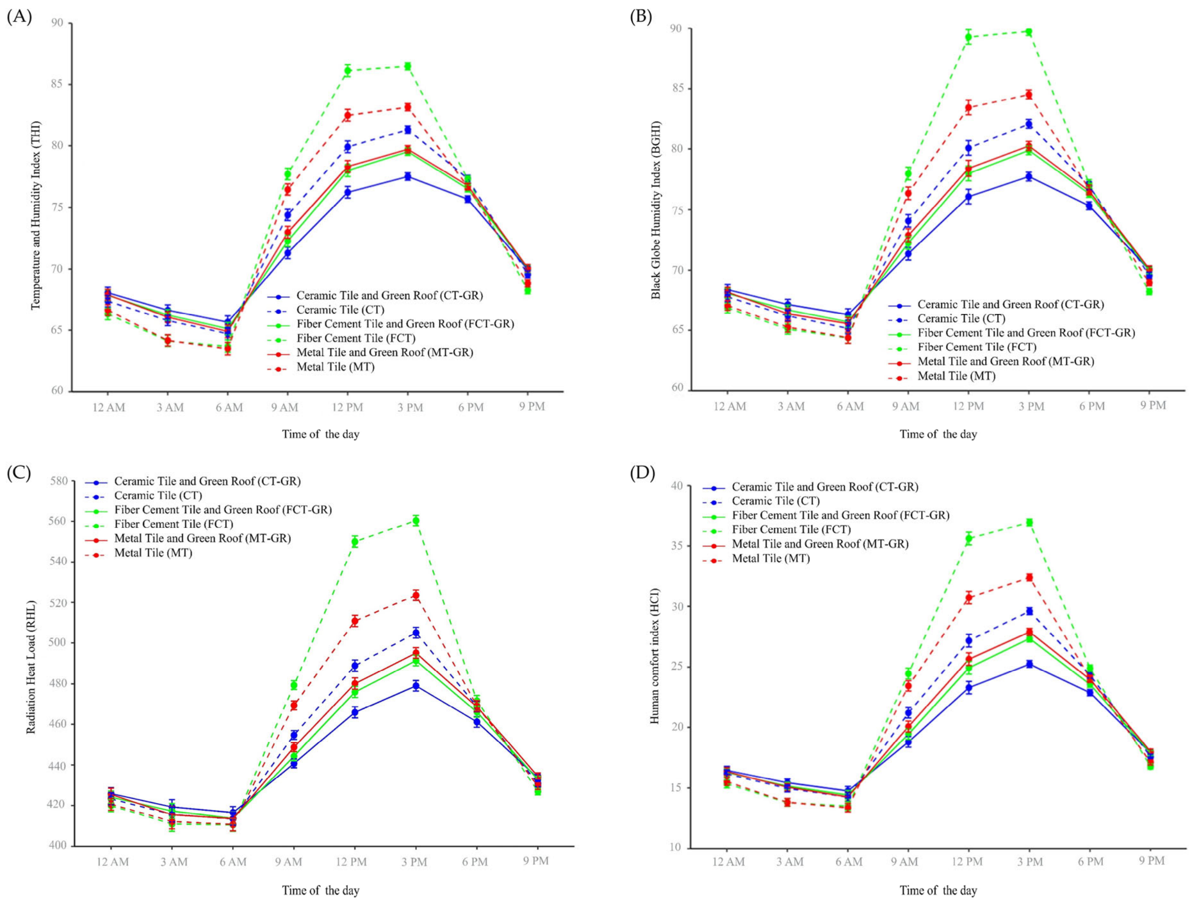

Figure 7. Behavior of the THI (**A**), BGHI (**B**), RTL (**C**), and HCI (**D**) in closed prototypes, demonstrating the effects of different types of roofing tiles, both with and without the presence of a green roof, at various time points. Source: Authors.

Closed prototype analysis (Figure 7B) revealed significant interactions (p-value < 0.0001) among almost all variables. Green roof presence resulted in substantial reductions in average BGHI values, particularly at 3:00 P.M., with the most pronounced reductions in prototypes with fiber cement tiles. During cooler times (6:00 P.M. to 06:00 A.M.), green roofs provided BGHI damping effects, though values remained higher compared to prototypes without green roofs. RTL analysis in closed prototypes (Figure 7C) showed significant interaction effects (p-value < 0.0001) among all variables. Green roof implementation reduced average RTL values during peak daytime temperatures, providing enhanced protection against incident solar radiation. HCI analysis in closed prototypes (Figure 7D) demonstrated interactions (p-value < 0.0001) among all variables. Prototypes with green roofs maintained lower HCI values and superior thermal conditions between 09:00 A.M. and 6:00 P.M. compared to those without green roofs.

4. Discussion

Given the characteristic climatic conditions at the experimental site and the varying experimental conditions of the prototypes (Figures 2 and 5), there is a clear need to adjust the thermal environment of the facilities to meet animal requirements, ensuring their thermal comfort and well-being [60]. Maintaining appropriate thermal comfort conditions is fundamental for efficient broiler production, requiring continuous adjustments in environmental variables [61,62]. Thermal management must adapt to both bird development and regional climatic variations. During the initial weeks, birds undergo environment acclimatization, while in later growth stages, increased body mass elevates the internal temperature of the shed, necessitating more stringent thermal control [62].

Furthermore, it is important to highlight that the ambient temperature is influenced not only by the roof but also by the walls of the installation. The characteristics of the walls, such as material and thickness, impact the retention and dissipation of heat, affecting the internal thermal environment. The side curtains of the prototypes, by functioning as a barrier to natural ventilation, allow the evaluation of treatments under controlled ventilation, providing a more precise analysis of the impact of thermal control on the internal environment.

When evaluating the broiler's life cycle in a real facility, it can be seen that the air temperature inside the prototypes (Figure 3A) remains at thermal comfort levels (Table 3) throughout the day, especially in the prototypes with the green roof. This configuration proved to be effective in mitigating heat gain, contributing to more stable indoor conditions suitable for animal welfare. On the other hand, at the hottest times of the day, the prototypes with fiber cement roofs had internal temperatures above the comfort limits, showing the unfavorable thermal impact of this material. Fiber cement roof tiles have intrinsic characteristics that limit their thermal performance, such as a thickness of 0.008 m, a specific heat of 0.84 kJ/kg.K, a density of 1900 kg/$m^{3,}$ and a heat capacity of 12.77 kJ/(m^2.K) [63]. These factors result in lower thermal inertia, leading the material to absorb and transfer heat quickly, in contrast to ceramic and metal tiles, which have greater thermal stability. In addition, the aging of fiber cement intensifies this effect since the darkening of the material increases its solar radiation absorption coefficient from 0.45 in new tiles to 0.80 in aged tiles [4,64]. This increase in heat absorption increases thermal discomfort, especially in environments with high solar incidence. During the critical hours of the day, the air temperature data in the open prototypes (Figure 3A) confirmed that fiber cement had the highest values, surpassing ceramic and metal tiles. This trend is attributed to the lower thermal inertia of fiber cement, which contributes significantly to the thermal instability observed [65].

The results observed in this study align with those found by Barnabé et al. [66], who reported similar air temperatures in prototypes with fiber cement roofing during peak heat hours, ranging from 32.0 to 35.0 °C between 12:00 P.M. and 3:00 P.M. This is consistent with the findings in northeastern Brazil, where they recorded maximum air temperatures of approximately 31.8 °C in calf housing with fiber cement roofing. Likewise, Oliveira et al. [53] evaluated fiber cement roofing in reduced-scale poultry house models and observed air temperatures around 33.0 °C, further confirming the trend observed in the present study. However, when comparing different roofing materials, Oliveira et al. [53] found that ceramic tiles provided superior solar radiation interception, with temperatures ranging from 30.6 °C to 31.6 °C, compared to fiber cement and metal tiles without additional roof protection. This supports the notion that ceramic tiles are more effective at functioning as thermal barriers, contributing to lower internal temperatures during peak heat periods. The findings from Oliveira et al. [53] and the present study emphasize the role of ceramic tiles in improving thermal comfort in animal production facilities, offering better insulation and minimizing temperature fluctuations, which can enhance animal welfare and productivity. In contrast, the higher air temperatures observed in prototypes with fiber cement roofing during peak heat hours suggest that this material is less effective in providing thermal insulation. This discrepancy may be attributed to the material's heat absorption properties, which are influenced by factors such as color, surface texture, and thermal mass. As a result, adjusting roofing materials or integrating additional protective measures, such as green roofing or reflective coatings, could be beneficial in improving the thermal performance of fiber–cement roofs and reducing internal temperatures.

Air temperature results in prototypes with lateral enclosure using ceramic tiles and green roofing (27.7 ± 0.5 °C), measured at 12:00 P.M. (Figure 5), were comparable to those reported by Carneiro et al. [31]. In their evaluation of green roofs in Pernambuco state using prototype poultry sheds with *Zoysia japonica* grass and peanuts (Arachis repens), they observed average internal air temperatures of approximately 27.7 °C for both plant species. Emphasizing the decisive role of selecting roofing materials that meet thermal comfort requirements is crucial, as they directly affect the internal microclimate and, consequently, the well-being and productivity of the animals housed. Green roofs, in particular, excel at stabilizing temperature fluctuations. By creating a more consistent indoor environment, they mitigate heat stress and provide optimal conditions for animal production, even under reduced ventilation. The comparison with the study by Carneiro et al. [31] reinforces the potential of green roofs as a sustainable and effective solution for improving thermal regulation in animal housing facilities.

In the present study [31], air temperature varied between 18.0 ± 0.3 °C and 30.5 ± 0.2 °C over the period of study in open prototypes with green roofing (Figure 3A), enabling an environment suitable for adult birds, which ranges between 18.0 and 28.0 °C in summer conditions with natural ventilation [11]. However, it is important to emphasize that the ideal thermal comfort conditions vary with the age of the birds. The selection of roofing materials must take thermal requirements into account in order to guarantee a favorable internal microclimate, directly impacting animal welfare and productivity. It should be noted that between the third and fourth week of production (Table 3), the comfortable air temperature range is 23.0 to 29.0 °C [67,68]. In this context, the green roof is an effective construction technique, promoting thermal comfort and internal temperature during these production phases.

The elevated air temperature inside the prototypes with side closure (Figure 6A) results in reduced air exchange between internal and external environments. This reduction allows the energy from incident solar radiation to increase internal air mass temperature, which remains trapped due to the lateral enclosures' limitation of air exchange. However, green can significantly reduce internal air temperature [69], as the vegetative cover minimizes temperature gains during periods of solar exposure.

Abreu et al. [67] established representative thermal comfort ranges for poultry throughout their reproductive cycle (Table 3): 29.0 to 32.0 °C in the second week and 20.0 to 23.0 °C in the fifth week. These ranges align with those observed in the present study, with the lowest values recorded in prototypes featuring green roofing and ceramic tiles. Air temperature analysis in prototypes revealed variation between 16 °C and 44 °C over the 24 h observation period (Figures 3A and 6A). The green roof prototypes maintained temperature within human comfort limits, according to La Roche et al. [16], who categorize thermal comfort in human dwellings into three levels: below 21.1 °C (cold), between 21.1 °C and 25.5 °C (comfortable), and above 25.5 °C (warm). The recorded temperature values indicate an environment with adequate thermal comfort for workers, conforming to Ministry of Labor and Employment standards [37].

Internal surface temperature analysis in the prototypes (Figures 3B and 6B) demonstrates that green roofing can significantly reduce thermal load in facilities, promoting a more suitable thermal environment for livestock. Pragati et al. [70] corroborate this finding, indicating that surface temperatures in buildings with green roofs are approximately 5.17% lower compared to conventional buildings without greening systems. Carneiro et al. [31] observed surface temperatures of approximately 36.7 °C on green roofs with *Zoysia japonica* grass, demonstrating the thermal efficiency of this vegetation cover compared to the present study's findings. Conversely, the elevated internal surface temperature (Figures 3B and 6B) in prototypes with fiber cement tiles without green roofing can be attributed to material darkening, which increases heat absorption from the external environment [64]. Additionally, Sampaio et al. [51], in a summer study conducted in southern Brazil, recorded lower fiber cement tile temperatures than those observed in this study without green roofing. This discrepancy can be explained by variations in climatic conditions, such as regional differences in temperature, humidity, and solar radiation, as well as the physical condition of the fiber cement roof tile. To optimize thermal performance in different climates, it can be beneficial to adjust or combine roofing materials, such as integrating green roofing or reflective coatings, to increase heat dissipation.

Beyond variations in internal surface temperature, it is crucial to relative humidity's impact on facility conditions. In the open prototype, relative humidity ranged between 40.8% and 74.3% (Figure 3C). These values are lower than those reported by Santos et al. [71], who documented monthly average relative humidity levels above 83.0% in poultry production environments in Sergipe. This difference can be attributed to their region's more humid coastal climate compared to the present experiment's location. Notably, prototypes with fiber cement roofing exhibited the lowest relative humidity levels during peak temperature periods between 12:00 P.M. and 3:00 P.M. (Figures 3C and 6C). This low relative humidity results from elevated air temperatures [72]. The green roof's substrate moisture retention likely contributed to increasing the relative humidity during peak heat periods, thereby improving environmental production conditions during these times. Relative humidity directly influences the thermal comfort and health of the animals. In the prototypes with green roofs (Figure 6C), humidity increased during the coldest hours due to evapotranspiration from the plants [70]. In prototypes closed on the sides, humidity exceeded 70%, regardless of the type of roof, which impairs the animals' transpiration, which can cause heat stress and respiratory diseases in the animals. Although green roofs improve the thermal conditions of the environment, it is necessary to balance the humidity when it is excessive. Ceramic tiles and fiber cement tiles have different characteristics: ceramic tiles dissipate heat better due to their greater thermal inertia [73], but they can retain more moisture, which favors condensation. Fiber cement tiles, on the other hand, absorb more heat, affecting the internal microclimate. Therefore, the combination of roofing materials and humidity control is fundamental to guaranteeing animal welfare. When well planned, the use of green roofs can promote a more balanced and healthier environment for animals.

The relative humidity values in the ceramic tile prototypes, both with and without green roofs, are particularly noteworthy (Figure 6C). Ceramic tiles' porosity enables environmental water absorption, contributing to their natural thermal performance by prolonging heat transmission [73]. However, this study's results indicate that ceramic tiles combined with green roofs promote higher relative humidity, which is potentially problematic in hot climates where it may compromise or impede air cooling processes. The disparity in mean values of relative humidity between the open and closed prototypes can be attributed to reduced ventilation in the internal environment and the effect of external airspeed, which removes heat from the surface of the tiles. Bollman et al. [15] reported similar findings, noting relative humidity changes due to water retention in green roof substrate, resulting in reduced internal building temperature. Despite variations, relative humidity values in green roof prototypes remained within the recommended range for poultry production (40.0% to 70.0%), as specified by Tinôco [52] and Ferreira [74]. Additionally, Bollman et al. [15] reported results similar to the present study (Figure 4), highlighting artificial reflective shadowing effects on relative humidity, with averages of 51.6% during the day and 72.7% at night in a tray system with a green roof in Corvallis, USA.

The results obtained in this study, when evaluating the thermal environment in prototypes with different types of roofing, made it possible to define thermal comfort indices (THI). In the prototypes with green roofs (Figure 4A), the average THI values provided optimal thermal comfort conditions, not only for the birds in the first week of life but throughout the production cycle, ranging from 72.0 to 80.0, as indicated by Silva et al. [50]. These values indicate that green roofs are effective in maintaining a comfortable environment for birds at different stages of growth [50]. In the prototypes without green roofs (Figure 7A), the THI approached the upper limit of this ideal range, with the fiber cement tile prototype exceeding the recommended range for broiler production [50]. This suggests that fiber cement roof tiles, because they do not have efficient thermal properties, contribute to an increase in internal temperature, compromising the birds' comfort, especially in warmer periods. This increase in temperature can lead to heat stress, negatively affecting the birds' performance [50]. These findings demonstrate that combining ceramic tiles with green roofing can enhance THI and consequently provide superior thermal comfort in the prototypes' internal environment. Passini et al. [75] identified average THI values similar to those found in the present study (Figures 4A and 7A), reaching an average of 77.0. Their study examined a broiler facility using reflective white paint on the external roof surface combined with artificial ventilation. However, the present study demonstrates that green roofing represents an effective alternative for promoting thermal comfort conditions; green roofs offer significant environmental and economic benefits, including reducing environmental impact through carbon sequestration and improving air quality. They also help retain moisture, reduce the need for irrigation, and reduce energy consumption by improving thermal efficiency and reducing reliance on artificial cooling systems. In economic terms, green roofs can reduce operational costs for ventilation and extend the life of the roof tiles, resulting in lower maintenance costs. This sustainable solution can, therefore, offer long-term benefits to producers, with potential government incentives and an appreciation of environmental commitment.

The thermal comfort analysis in reduced models demonstrates that green roofing can create a more thermally suitable environment for broilers, with results comparable to conventional methods such as combining white reflective paint with artificial ventilation [75]. However, Carneiro et al. [31], studying green roofs on reduced models of livestock facilities in Pernambuco state, observed average THI values around 26.0 for both peanut grass (Arachis repens) and *Zoysia japonica* grass. These values differ from the present study's findings, likely due to regional microclimatic variations.

These findings indicate that green roofing represents an effective construction technique with potential application in full-scale facilities. However, further detailed studies are needed to evaluate its practical implications for improving thermal conditions in animal production environments. As a sustainable alternative to conventional techniques, green roofing can significantly contribute to thermal comfort, reinforcing its value as an efficient and environmentally responsible solution.

Investigating green roof effects on BGHI during nighttime hours (6:00 P.M. to 06:00 A.M.) highlights the remarkable thermal insulation capacity of ceramic tiles with green covering, maintaining average BGHI values above other treatments (Figure 4B). The green roof's influence on BGHI is particularly evident during peak heat hours (9:00 A.M. to 3:00 P.M.), where average values in prototypes with this roofing reached 68.0 and 81.0 at 12:00 P.M. and 3:00 P.M. respectively, within the established thermal comfort range for broiler chickens, according to Oliveira et al. according to Oliveira et al. [52].

Furthermore, analysis of BGHI behavior in green ceramic tile prototypes without green roofing revealed values similar to those with metallic tiles and roofs (Figure 7B). Comparing this study's BGHI values with those documented by Oliveira et al. (2006) suggests that green roofing may enhance animal thermal comfort based on established BGHI values for adult-phase animals. Moreover, Sampaio et al. [51] observed an average BGHI value of approximately 80.2 in poultry house prototypes with lateral enclosures using ceramic tile roofing at 12:00 P.M., exceeding the animals' comfort range. This value closely mirrors the BGHI value obtained from identical tiles in the present investigation [73] Oliveira et al. (2006) [51] (Figure 7B).

Sampaio et al. [51], researching scaled-down animal production facility models, assert that vegetative roofing can induce cold stress, with an average BGHI of 70.0 varying by time of day and season. This contrasts with the higher mean BGHI values observed in green roof prototypes in the present study, which promote thermal comfort conditions (Figures 4B and 7B). Buffington et al. [35] establish that BGHI values up to 74.0 indicate comfort, while values above 84.0 signal emergency conditions for animal production, including poultry, cattle, and swine. The present study's results demonstrate that green roofs can provide a thermal environment conducive to animal requirements, potentially facilitating natural thermal conditioning within facilities [35].

Similarly, research by Sampaio et al. [51] reported that animal production facilities could achieve approximately 40.0% air temperature reduction during peak heat periods, consistent with this study's findings. However, green roofing led to even greater air temperature reductions (Figure 4C). The effectiveness of air temperature reduction varies with tile type when combined with green covering due to differing physical characteristics and thermal properties of materials. In enclosed prototypes (Figure 7C), green roofing also reduced average RTL values during peak heat periods, providing enhanced protection against incident solar radiation. The RTL values obtained in this study for prototypes with ceramic tiles and green roofs under both open and closed conditions (Figure 1) were comparable to those reported by Sampaio et al. [51]. They documented RTL values in Southern Brazil ranging from 406.7 to 479.2 W/m^2 for ceramic-tiled prototypes during winter and summer. Passini et al. [75] observed that white-painted roofing with artificial ventilation could reduce RTL by approximately 6.4 W/m^2. However, the current study demonstrated more substantial reductions in green-roofed prototypes. Notably, in enclosed prototypes with fiber cement tiles, the difference between those with and without green roofs was 74.0 W/m^2 at 12:00 P.M. and 69.0 W/m^2 at 3:00 P.M. (Figure 7C) [51,75]. The combination of ceramic tiles with a green roof has proven to be the most efficient in regulating the indoor microclimate, providing a significant improvement in thermal conditions. The combination of fiber cement tiles with a green roof, although less effective, still presents considerable benefits in mitigating heat. The use of green roofs combined with tiles with adequate thermal characteristics constitutes an effective strategy for optimizing thermal comfort and, consequently, animal welfare in production facilities, promoting a more stable environment that is favorable to productive performance.

Worker thermal environment assessment is essential, as it directly impacts health, well-being, and productivity [37]. This index provides a scientific basis for monitoring and adjusting environmental conditions within ideal comfort limits for specific activities, ensuring an adequate and safe workspace. In open prototypes, average HCI values without green roofing (Figure 4D) were higher during peak heat hours (9:00 A.M. to 3:00 P.M.), with notable peaks in fiber cement tile prototypes. However, during nighttime hours (6:00 P.M. to 6:00 A.M.), ceramic tiles with green covering demonstrated superior thermal insulation capacity, maintaining HCI above other treatments (Figure 4D).

Treatment disparities can be attributed to roofing materials' thermal properties [64]. Tiles without green covering protection tend to absorb more heat compared to covered tiles, which directly intercept solar radiation. This variation is crucial, particularly during peak heat hours when average HCI values approach 40.0 (Figure 7D), indicating uncomfortable worker conditions. Considering average HCI values in green-roofed prototypes, regardless of tile type (Table 2), this feature clearly provides comfortable worker conditions. This finding emphasizes green roofs' importance in promoting thermal comfort for both animals and facility workers.

5. Conclusions

Green roof implementation in animal production facilities has proven effective in enhancing the internal thermal environment, reducing temperature peaks, and promoting comfort—essential factors for animal welfare. This study's results demonstrate that green roofing, regardless of tile type, reduced indoor air temperature by up to 2.4 °C in open prototypes and 10.6 °C in closed prototypes during peak heat hours (3:00 P.M.). A significant reduction in the internal surface temperature of fiber cement tiles was also observed, reaching up to 24.0 °C in open prototypes and 27.0 °C in closed ones. The thermal comfort indexes (THI, BGHI, and RTL) also showed reductions, indicating green roofing's effectiveness in heat mitigation. The HCI for both types of green roof prototypes indicated comfortable conditions, complying with Ministry of Labor and Employment legislation.

Green roofs' natural thermal insulation reduces artificial cooling system requirements and represents a sustainable alternative for mitigating climate change effects on production facilities. Despite technical and financial challenges, including installation and maintenance costs, the environment and thermal comfort benefits justify increased investment and research to adapt this technology to agricultural applications, particularly in hot climates where thermal control is essential for animal production.

This study makes an innovative contribution by demonstrating, through experimental data, the thermal benefits of green roofs in reduced-scale poultry house prototypes. Green roof application in animal production facilities offers a viable solution for improving thermal conditions in these environments. The results provide valuable insights for future green roof implementation in the agricultural sector and can serve as a foundation for further research focused on enhancing thermal comfort and mitigating climate change impacts in rural animal production facilities.

Finally, carrying out analyses on reduced models of agricultural facilities is essential to assess the feasibility and performance of innovative technologies, such as green roofs, under controlled conditions before large-scale implementation. This approach enables a better understanding of thermal impacts, refinement of design parameters, and more precise estimation of costs and benefits, facilitating informed decisions that optimize thermal comfort and sustainability in animal production facilities.

Author Contributions: M.A.d.S.: Conceptualization, Data curation, Investigation, Methodology, Visualization, Writing—original draft, Writing—review and editing. F.C.d.S.: Conceptualization, Funding acquisition, Project administration, Resources, Supervision, Writing—review and editing. A.L.d.S.: Formal analysis, Software, Validation, Visualization. T.C.S.: Investigation, Methodology. C.P.O.: Investigation, Methodology. R.B.V.: Supervision, Writing—review and editing. F.d.C.B.: Conceptualization, Supervision, Writing—review and editing. I.d.F.F.T.: Resources, Supervision, Writing—review and editing. All authors have read and agreed to the published version of the manuscript.

Funding: This research was partially funded by the Coordination for the Improvement of Higher Education Personnel—Brazil (CAPES)—Financial Code 001.

Data Availability Statement: The data will be available upon request.

Acknowledgments: To the Research Center for Ambience and Agroindustrial Systems Engineering (AMBIAGRO) within the Department of Agricultural Engineering at the Federal University of Viçosa (UFV), to the Coordination for the Improvement of Higher Education Personnel, Brazil, (CAPES) with Financial Code 001, to the National Council for Scientific and Technological Development, Brazil (CNPq), and to the Minas Gerais Research Support Foundation, Brazil (FAPEMIG), we extend our sincere gratitude for the support provided.

Conflicts of Interest: The authors declare no conflicts of interest.

Symbols and Abbreviations

$W \cdot (m^2 \cdot K^4)^{-1}$—watts per square meter per kelvin to the fourth power, $m \cdot s^{-1}$—meters per second, K—kelvin, %—percent, kPa—kilopascals, °C—degrees Celsius, m^2—square meters, Air Temperature—(AT), Relative Humidity—(RH), Temperature and Humidity Index—(THI), Black Globe Humidity Index—(BGHI), Human Comfort Index—(HCI), Radiant Thermal Load—(RTL), Ceramic Tile—(CT), Fiber Cement Tile—(FCT), Metal Tile—(MT), Ceramic Tile with Green Roof—(GCT), Fiber Cement Tile with Green Roof—(GFT), Metal Tile with Green Roof—(GMT), Crop Evapotranspiration—(ETc), Reference Evapotranspiration—(ET0).

References

1. ABPA. Associação Brasileira de Proteína Animal. 2023, pp. 1–75. Available online: https://abpa-br.org/ (accessed on 22 April 2024).
2. ABPA. Associação Brasileira de Proteína Animal. 2024, pp. 1–77. Available online: https://abpa-br.org/wp-content/uploads/2024/04/ABPA-Relatorio-Anual-2024_capa_frango.pdf (accessed on 22 April 2024).
3. Mascarenhas, N.M.H.; da Costa, A.N.L.; Pereira, M.L.L.; de Caldas, A.C.A.; Batista, L.F.; Andrade, E.L.G.; Mascarenhas, N.M.H.; da Costa, A.N.L.; Pereira, M.L.L.; de Caldas, A.C.A.; et al. Thermal conditioning in the broiler production: Challenges and possibilities. *J. Anim. Behav. Biometeorol.* **2020**, *6*, 52–55. [CrossRef]
4. Gonçalves, I.C.M.; Turco, S.H.N.; Neto, J.P.L.; Nascimento, J.W.B.D.; de Lima, V.L.A.; Borges, V.P. Thermal performance of aviary located in the semiarid region of Pernambuco based on computer simulation. *Rev. Bras. Eng. Agric. Ambient.* **2022**, *26*, 533–540. [CrossRef]
5. Mottet, A.; Tempio, G. Global poultry production: Current state and future outlook and challenges. *Worlds Poult. Sci. J.* **2017**, *73*, 245–256. [CrossRef]
6. Cheng, M.; McCarl, B.; Fei, C. Climate Change and Livestock Production: A Literature Review. *Atmosphere* **2022**, *13*, 140. [CrossRef]
7. Syarifuddin, H.; Sy, A.R.; Devitriano, D. CH4 Gas Mitigation Strategy with the Use of Interpretative Structural Modeling Method. In Proceedings of the 3rd Green Development International Conference (GDIC 2020); Atlantis Press: Amsterdam, The Netherlands, 2021; Volume 205, pp. 474–481. [CrossRef]
8. IPCC. *2014: Synthesis Report. Contribution of Working Groups I, II and III to the Fifth Assessment Report of the Intergovernmental Panel on Climate Change*; Core Writing Team, Pachauri, R.K., Meyer, L.A., Eds.; IPCC: Geneva, Switzerland, 2014.
9. Melo, T.V.; Furlan, R.L.; Milani, A.P.; Buzanskas, M.E.; de Moura, A.M.A.; Mota, D.A. Roof pitch and exposure and different roofing materials in reduced models of animal production facilities in the fall and winter. *Rev. Bras. Saúde Produção Anim.* **2015**, *16*, 658–666. [CrossRef]
10. Andric, I.; Kamal, A.; Al-Ghamdi, S.G. Efficiency of green roofs and green walls as climate change mitigation measures in extremely hot and dry climate: Case study of Qatar. *Energy Rep.* **2020**, *6*, 2476–2489. [CrossRef]
11. Baêta, F.C.; Souza, C.F. *Ambiência em Edificações Rurais: Conforto Animal*, 2nd ed.; UFV: Viçosa, Brazil, 2010.
12. Damasceno, F.A.; Schiassi, L.; Yanagi, T.; Osorio-Saraz, J.A.; Oliveira, J.L.-D. Evaluación térmica de tejas ecologicas en modelos físicos de galpones avicolas. *DYNA* **2016**, *83*, 114–119. [CrossRef]
13. Sampaio, C.A.P.; Terezo, R.F.; Motta, G.; Silva, L.M.C.; Júnior, I.V. Environmental thermal comfort of a reduced model using cross-laminated timber. *Eng. Agrícola* **2020**, *40*, 413–419. [CrossRef]
14. Shafique, M.; Kim, R.; Rafiq, M. Green roof benefits, opportunities and challenges—A review. *Renew. Sustain. Energy Rev.* **2018**, *90*, 757–773. [CrossRef]
15. Bollman, M.A.; DeSantis, G.E.; Waschmann, R.S.; Mayer, P.M. Effects of shading and composition on green roof media temperature and moisture. *J. Environ. Manag.* **2021**, *281*, 111882. [CrossRef]
16. La Roche, P.; Yeom, D.J.; Ponce, A. Passive cooling with a hybrid green roof for extreme climate. *Energy Build.* **2020**, *224*, 110243. [CrossRef]
17. Krebs, L.F.; Johansson, E. Influence of microclimate on the effect of green roofs in Southern Brazil—A study coupling outdoor and indoor thermal simulations. *Energy Build.* **2021**, *241*, 110963. [CrossRef]
18. Boafo, F.E.; Kim, J.T.; Kim, J.H. Evaluating the impact of green roof evapotranspiration on annual building energy performance. *Int. J. Green Energy* **2017**, *14*, 479–489. [CrossRef]
19. La Roche, P.; Berardi, U. Comfort and energy savings with active green roofs. *Energy Build.* **2014**, *82*, 492–504. [CrossRef]
20. Theodosiou, T. Green Roofs in Buildings: Thermal and Environmental Behaviour. *Adv. Build. Energy Res.* **2009**, *3*, 271–288. [CrossRef]

21. Lazzarin, R.M.; Castellotti, F.; Busato, F. Experimental measurements and numerical modelling of a green roof. *Energy Build.* **2005**, *37*, 1260–1267. [CrossRef]
22. Sailor, D.J.; Elley, T.B.; Gibson, M. Exploring the building energy impacts of green roof design decisions-a modeling study of buildings in four distinct climates. *J. Build. Phys.* **2012**, *35*, 372–391. [CrossRef]
23. Droz, A.G.; Coffman, R.R.; Blackwood, C.B. Plant diversity on green roofs in the wild: Testing practitioner and ecological predictions in three midwestern (USA) cities. *Urban For. Urban Green* **2021**, *60*, 127079. [CrossRef]
24. Sultana, M.N.; Akib, S.; Ashraf, M.A. Thermal comfort and runoff water quality performance on green roofs in tropical conditions. *Geol. Ecol. Landsc.* **2017**, *1*, 47–55. [CrossRef]
25. Yang, Y.; Davidson, C.I.; Zhang, J. Evaluation of thermal performance of green roofs via field measurements and hygrothermal simulations. *Energy Build.* **2021**, *237*, 110800. [CrossRef]
26. Houchmand, L.J.; Martí, M.M.; Gassó-Domingo, S. Photovoltaics and green roofs: Holistic analysis in built environments. *Renew. Sustain. Energy Rev.* **2025**, *207*, 114987. [CrossRef]
27. Yan, J.; Yang, P.; Wang, B.; Wu, S.; Zhao, M.; Zheng, X.; Wang, Z.; Zhang, Y.; Fan, C. Green Roof Systems for Rainwater and Sewage Treatment. *Water* **2024**, *16*, 2090. [CrossRef]
28. Jamei, E.; Chau, H.W.; Seyedmahmoudian, M.; Mekhilef, S.S.; Sami, F.A. Green roof and energy—Role of climate and design elements in hot and temperate climates. *Heliyon* **2023**, *9*, e15917. [CrossRef] [PubMed]
29. Kostadinović, D.; Jovanović, M.; Bakić, V.; Stepanić, N. Mitigation of urban particulate pollution using lightweight green roof system. *Energy Build.* **2023**, *293*, 113203. [CrossRef]
30. Talwar, P.; Verma, N.; Khatri, H.; Ahire, P.D.; Chaudhary, G.; Lindenberger, C.; Vivekanand, V. A systematic review of photovoltaic-green roof systems in different climatic conditions focusing on sustainable cities and societies. *Sustain. Cities Soc.* **2023**, *98*, 104813. [CrossRef]
31. Carneiro, T.A.; Guiselini, C.; Pandorfi, H.; Neto, J.P.L.; Loges, V.; de Souza, R.F.L. Condicionamento térmico primário de instalações rurais por meio de diferentes tipos de cobertura. *Rev. Bras. Eng. Agrícola Ambient.* **2015**, *19*, 1086–1092. [CrossRef]
32. Souza, M.A.; Sousa, F.C.; Baêta, F.C.; Vigoderis, R.B.; Zanetoni, H.H.R. Green roofs in animal production facilities—A review of strategies for estimating the carbon dioxide balance. *Renew. Sustain. Energy Rev.* **2024**, *189*, 114000. [CrossRef]
33. Thom, E.C. The Discomfort Index. *Weatherwise* **1959**, *12*, 57–61. [CrossRef]
34. Mader, T.L.; Davis, M.S.; Brown-Brandl, T. Environmental factors influencing heat stress in feedlot cattle. *J. Anim. Sci.* **2006**, *84*, 712–719. [CrossRef]
35. Buffington, D.E.; Collazo-Arocho, A.; Canton, G.H.; Pitt, D.; Thatcher, W.W.; Collier, R.J. Black globe-humidity index (BGHI) as comfort equation for dairy cows. *Elibrary. Asabe.Org.* **1981**, *24*, 711–0714. [CrossRef]
36. Rosenberg, V.S.B. *Microclimate: The Biological Environment*; John Wiley & Sons: New York, NY, USA, 1983.
37. Lei nº 6.514, de 22 de dezembro de 1977. Altera o Capítulo V, Título II, da Consolidação das Leis do Trabalho, relativa à Segurança e Medicina do Trabalho. Diário Oficial da União, Brasília, DF, 23 dez. 1977. Available online: https://legislacao.presidencia.gov.br/ (accessed on 22 April 2024).
38. Kelly, C.F.; Bond, T.E. Effectiveness of artificial shade materials. *Agric. Eng.* **1958**, *39*, 758–764.
39. Jentzsch, R.; Costa Baêta, F.; Tinôco, I.F.F.; Damasceno, F.A.; Cecon, P.R.; Saraz, J.A.O. Previsão de parâmetros térmicos ambientais dentro de modelos físicos em escala reduzida de alojamentos avícolas. *Interciencia* **2011**, *36*, 738–742. Available online: https://www.researchgate.net/publication/291497349 (accessed on 30 October 2024).
40. de Castro, A.C.; da Silva, I.J.O.; Nazareno, A.C.; Nunes, M.L.A.; Piedade, S.M.d.S. Thermal Efficiency of Different Coverage Materials in Reduced Models of Animal Husbandry Facilities: A Case Study. *Eng. Agrícola* **2017**, *37*, 403–413. [CrossRef]
41. Jentzsch, R.; Baêta, F.C.; Tinôco, I.F.F.; Damasceno, F.A.; Saraz, J.A.O. Parâmetros Arquitetônico-Ambientais para Construção e Testes em Modelos Reduzidos, Representativos de Galpões Avícolas, com Base em Similitude. *Rev. Eng. Agric.* **2013**, *21*, 19–30. [CrossRef]
42. Murphy, G. *Similitude in Engineering*; The Tonald Press Company: New York, NY, USA, 1950.
43. Bôas, R.L.V.; de Godoy, L.J.G.; Backes, C.; Santos, A.J.M.D.; Carribeiro, L.S. Sod production in Brazil. *Ornam. Hortic.* **2020**, *26*, 516–522. [CrossRef]
44. Martin, P.M. The potential of native grasses for use as managed turf. In Proceedings of the 4th International Crop Science Congress; CDROM: Brisbane, Australia, 2004; p. 13. Available online: https://www.cropscience.org.au (accessed on 25 October 2024).
45. Associação Nacional Grama Legal, Grama Esmeralda—Zoysia Japônica 2024. Available online: https://gramalegal.com/grama-esmeralda (accessed on 24 October 2024).
46. Rodríguez, J.; Vilela, K. Influence of the Types of Grass of Green Roofs for the Design of Thermal Comfort in Buildings. *J. Ecol. Eng.* **2022**, *23*, 223–229. [CrossRef]
47. Allen, R.; Pereira, L.; Raes, D.; Fao, M.S.; Rome, U. *Crop Evapotranspiration-Guidelines for Computing Crop Water Requirements-FAO Irrigation and Drainage Paper 56*; Food and Agriculture Organization of the United Nations: Rome, Italy, 1998.
48. INMET. 2022. Available online: https://tempo.inmet.gov.br/TabelaEstacoes/A510 (accessed on 19 July 2022).

49. Madeira, A.P.; Beneditto, D.; Doutor, S.S.; Zoologia, E. Necessidades hídricas das gramas batatais (Paspalum notatum Flüggé) e esmeralda (Zoysia Japônica Steud)estimadas por sensoriamento remoto. *Braz. J. Dev.* **2021**, *6*, 73015–73024.
50. Silva, E.T.d.; Leite, D.G.; Yuri, F.M.; Nery, F.d.S.G.; Rego, J.C.C.; Zanatta, R.d.A.; Santos, S.A.d.; Moura, V.V. Determinação do Índice de Temperatura e Umidade (ITU) para produção de aves na mesorregião metropolitana de Curitiba—PR. *Rev. Acadêmica Ciências Agrárias Ambient.* **2004**, *2*, 47–60.
51. Sampaio, C.A.P.; Cardoso, C.O.; Souza, G.P. Temperatura superficiais de telhas e sua relação com o ambiente térmico. *Eng. Agric.* **2011**, *31*, 1–11. [CrossRef]
52. Oliveira, R.F.M.; Donzele, J.L.; De Abreu, M.L.T.; Ferreira, R.A.; Vaz, R.G.M.V.; Cella, P.S. Effects of temperature and relative humidity on performance and yield of noble cuts of broilers from 1 to 49 days old. *Rev. Bras. Zootec.* **2006**, *35*, 797–803. [CrossRef]
53. Oliveira, C.P.; de Sousa, F.C.; Dallago, G.M.; Silva, J.R.; Campos, P.H.R.F.; Guimarães, M.C.d.C.; Baêta, F.d.C. Thermal Environment and Animal Comfort of Aviary Prototypes with Photovoltaic Solar Panel on the Roof. *Energies* **2023**, *16*, 2504. [CrossRef]
54. Brauer-Vigoderis, R.; Ferreira-Tinôco, I.D.F.; Pandorfi, H.; Bastos-Cordeiro, M.; De Souza-Júnior, J.P.; De Carvalho-Guimarães, M.C. Effect of heating systems in litter quality in broiler facilities in winter conditions. *Dyna* **2014**, *81*, 36. [CrossRef]
55. Carvalho, F.B.; Sartori, J.R.; Pezzato, A.C.; Fascina, V.B.; Castelo, P.G.; De Souza, I.M.G.P. Environmental temperature and broiler age on corn energy value. *Ciência Anim. Bras.* **2021**, *22*, e65526. [CrossRef]
56. Santos, W.M.M. *Índices de Conforto e Desconforto Térmico Humano segundo os Cenários Climáticos Do IPCC*; Congresso Brasileiro de Meteorologia: Belém, Brazil, 2010; p. 16.
57. de Souza, D.M.; Nery, J.T. O conforto térmico na perspectiva da Climatologia Geográfica. *GEOGRAFIA* **2012**, *21*, 65–83. [CrossRef]
58. Santos, G.; Miranda, B.; Diniz, F.R.; Da Silva, M.P. Avaliação e comparação do índice de conforto térmico humano entre as cidades de São Paulo (SP) e Bauru (SP). *J. Contrib.* **2017**, 1–5. [CrossRef]
59. TEAM, R.C.R. *R: A Language and Environment for Statistical Computing, 4.0.4 Los ed.*; R Foundation for Statistical Computing: Vienna, Austria, 2021.
60. Tinôco, I. Avicultura Industrial: Novos Conceitos de Materiais, Concepções e Técnicas Construtivas Disponíveis para Galpões Avícolas Brasileiros. *Rev. Bras. Cienc. Avic.* **2001**, *3*, 1–26. [CrossRef]
61. Collier, R.J.; Gebremedhin, K.G. Thermal Biology of Domestic Animals. *Annu. Rev. Anim. Biosci.* **2015**, *3*, 513–532. [CrossRef]
62. Pereira, F.; Ferreira, J.C.; Campos, A.T.; Ferreira, P.; Ferraz, P.; Bahuti, M.; Junior, T.Y.; Da Silva, J.P.; Ferreira, S.C. Dynamics of the Thermal Environment in Climate-Controlled Poultry Houses for Broiler Chickens. *Agriengineering* **2024**, *6*, 3891–3911. [CrossRef]
63. Michels, C.; Güths, S.; Marinoski, D.L.; Lamberts, R. Thermal performance and thermal resistance of fibre cement roof tiles: Experimental study. *Energy Build.* **2021**, *231*, 110569. [CrossRef]
64. Rivero, R. *Arquitetura e Clima: Acondicionamento Térmico Natural*, 2nd ed.; Rev. e Ampl.: Porto Alegre, RS, Brazil, 1986.
65. Verbeke, S.; Audenaert, A. Thermal inertia in buildings: A review of impacts across climate and building use. *Renew. Sustain. Energy Rev.* **2018**, *82*, 2300–2318. [CrossRef]
66. Barnabé, J.M.C.; Pandorfi, H.; de Almeida, G.L.P.; Guiselini, C.; Jacob, A.L. Temperatura superficial de materiais utilizados para cobertura individual de bezerreiros. *Rev. Bras. Eng. Agrícola Ambient.* **2014**, *18*, 545–550. [CrossRef]
67. Abreu, V.M.N.; de Abreu, P.G. Os desafios da ambiência sobre os sistemas de aves no Brasil. *Rev. Bras. Zootec.* **2011**, *40*, 1–14.
68. Cândido, M.G.; Tinôco, I.D.F.; Pinto, F.D.A.D.C.; Santos, N.T.; Roberti, R.P. Determination of thermal comfort zone for early-stage broilers. *Eng. Agrícola* **2016**, *36*, 760–767. [CrossRef]
69. Faggianelli, G.A.; Brun, A.; Wurtz, E.; Muselli, M. Natural cross ventilation in buildings on Mediterranean coastal zones. *Energy Build.* **2014**, *77*, 206–218. [CrossRef]
70. Pragati, S.; Priya, R.S.; Pradeepa, C.; Senthil, R. Simulation of the Energy Performance of a Building with Green Roofs and Green Walls in a Tropical Climate. *Sustainability* **2023**, *15*, 2006. [CrossRef]
71. Santos, G.D.B.; Sousa, I.F.D.; Brito, C.O.; Santos, V.D.S.; Barbosa, R.D.J.; Soares, C. Estudo bioclimático das regiões litorânea, agreste e semiárida do estado de Sergipe para a avicultura de corte e postura. *Ciência Rural.* **2014**, *44*, 123–128. [CrossRef]
72. Steadman, R.G. The Assessment of Sultriness. Part I: A Temperature-Humidity Index Based on Human Physiology and Clothing Science. *J. Appl. Meteorol. Climatol.* **1979**, *18*, 861–873. [CrossRef]
73. Bueno, A.D. Transferência de Calor e Umidade em Telhas: Simulação e Análise Experimental. Doctoral Dissertation, Universidade Federal de Santa Catarina, Florianópolis, Brazil, 1994.
74. Ferreira, R.A. *Maior Produção com Melhor Ambiente Para aves, Suínos e Bovinos*; Aprenda Fácil: Viçosa, Brazil, 2005.
75. Passini, R.; de Araújo, M.A.G.; Yasuda, V.M.; Almeida, E.A. Intervenção ambiental na cobertura e ventilação artificial sobre índices de conforto para aves de corte. *Rev. Bras. Eng. Agrícola Ambient.* **2013**, *17*, 333–338. [CrossRef]